Executive Summary

Feasibility of using nanotechnology to improve TIR satellite imagers

ESTEC contract number 4000104986/11/NL/CBi

Document number	PR-6813-07
Document version	1.0
Issue date	11th April 2013

Written by	Peter Hargrave Phil Buckle	Cardiff University
	Peter Vines Chee Hing Tan Siew Li Tan	Sheffield University
	Neil Gordon	Malvern Labs
	Les Hipwood Peter Knowles	Selex Gallileo
Approved by	Peter Hargrave Nick Nelms	Cardiff University European Space Agency

CARDIFF UNIVERSITY
PRIFYSGOL CAERDYDD

The University Of Sheffield.

Malvern Labs

SELEX GALILEO
A Finmeccarica Company

1. Introduction 5

1.1. Purpose 5

1.2. Scope 5

1.3. Applicable and reference documents 5

1.3.1. Applicable documents 5

1.3.2. Reference documents 5

1.4. Acronyms 6

2. Summary of Quantum Dot Infrared Photodetector technology 7

2.1. Current performance and future potential 7

3. Summary of Type-II superlattice detector technology 9

3.1. Current performance and future potential 9

4. Comparison of TIR detector technologies 11

4.1. Cost 11

4.2. Uniformity 11

4.3. Dark current 13

4.4. Detectivity 13

5. Feasibility of using QDIP or T2SL arrays for satellite-based TIR focal plane arrays 14

Technology roadmap 15

5.1. High-level pictorial roadmaps 15

5.2. Roadmapping summary 19

6. References 21

1. Introduction

1.1. Purpose

This document is the executive summary for a study carried out under ESTEC contract number 4000104986/11/NL/CBi "Feasibility of using nanotechnology to improve TIR satellite imagers.

The original objectives of the activity were:

I. To assess the current state-of-the-art in space detector equipment miniaturisation (including nano-technologies e.g. QDIP, QWIP) for thermal infrared applications.
II. To assess the feasibility of using, and potential performance of quantum dot infrared photodetectors (QDIP) for space applications.
III. To identify potential technology developments in order to implement space-borne QDIPs.
IV. Establish a roadmap for space application and qualification of QDIPs.

By the time of the mid-term review, it had been established that type-II superlattice (T2SL) detector technology held as much, if not more potential as QDIP technology. The remainder of the study was carried out with a focus on T2SL technology, in addition to the planned QDIP study.

This document presents the key findings and recommendations of this study. For more details, the reader is referred to the study final report [RD-5]

1.2. Scope

This document is a formal deliverable of the above-mentioned feasibility study. It is a public document.

1.3. Applicable and reference documents

1.3.1. Applicable documents

[AD-1] ESA statement of work "Feasibility of using nanotechnology to improve TIR satellite imagers". Appendix to AO/1-6813/11/NL/AF. Document reference TEC-MXX/2011/158. Issue 1, revision 1. 24/05/2011

1.3.2. Reference documents

[RD-1] TIR technology review report (D1) – ESA contract 4000104986/11/NL/CBi "Feasibility of using nanotechnology to improve TIR satellite imagers".

[RD-2] TIR FPA requirements analysis report (D2) – ESA contract 4000104986/11/NL/Cbi "Feasibility of using nanotechnology to improve TIR satellite imagers".

[RD-3] QDIP and T2SL performance assessment report (D3) – ESA contract 4000104986/11/NL/Cbi "Feasibility of using nanotechnology to improve TIR satellite imagers".

[RD-4] TIR FPA roadmap report (D4) – ESA contract 4000104986/11/NL/Cbi "Feasibility of using nanotechnology to improve TIR satellite imagers".

[RD-5] Final report – ESA contract 4000104986/11/NL/Cbi "Feasibility of using nanotechnology to improve TIR satellite imagers".

1.4. Acronyms

BLIP	Background Limited Performance
DWELL	Dots in a well
FPA	Focal Plane Array
FPN	Fixed Pattern Noise
IR	Infrared
LWIR	Long Wave Infrared
MPC	Metal Photonic Crystal
MWIR	Medium Wave Infrared
QD	Quantum Dot
QDIP	Quantum Dot Infrared Photodetector
QE	Quantum Efficiency
QW	Quantun Well
QWIP	Quantum Well Infrared Photodetector
ROIC	Readout Integrated Circuit
SLS	Strained Layer Superlattice
SWIR	Short Wave Infrared
T2SL	Type-II superlattice
TIR	Thermal Infrared
VLWIR	Very Long Wave Infrared

2. Summary of Quantum Dot Infrared Photodetector technology

2.1. Current performance and future potential

A thorough review of QDIP FPA performance has been conducted, and a summary of state-of-the-art performance figures is presented in Table 1. QDIP FPAs show modest performance at present which does not exceed other TIR technologies such as QWIPs and HgCdTe FPAs. It has been predicted that QDIP FPAs have the potential to exceed QWIP performance and rival HgCdTe performance [1, 2] if significant QD growth challenges can be overcome. These challenges include growing QDIPs with QDs which are uniform in size and shape and with optimised doping. These growth improvements would increase the carrier lifetime and could lead to improved device performance as a result. However, it should be stressed that the projected performance figures quoted in these papers can only be used as a guide until the lifetime parameters used are confirmed experimentally.

Looking at array size, we note that 2048x2048 InSb and HgCdTe arrays exist [3, 4] and HgCdTe array sizes up to 4096x4096 (16 megapixels) are under development [4]. These arrays are fabricated using processes similar to those that would be used for large QDIP FPAs so there will be no fundamental barriers to expanding QDIP array size to several megapixels. Importantly, QDIPs benefit from mature III-V growth with established GaAs substrates currently available up to 8 inches in diameter [5]. The growth of large-area wafers for megapixel FPAs will not be problematic.

An interesting feature of QDIP arrays is the possibility of exploiting the bias tuneability of the spectral response, which would present an advantage over HgCdTe detectors and QWIPs. It has been possible to use multi band voltage tuneable QDIPs combined with a post processing algorithm for multispectral detection and spectroscopy [6, 7]. Figure 1 has been reproduced from reference [7] and shows a reasonable reconstruction of a polyethylene sheet throughout the MWIR and LWIR ranges indicating spectral features as narrow as 0.3µm. If this system can be integrated with an FPA, two dimensional chemical classification and spectroscopy should be possible without optical filters. If a greater control over QDIP growth can be attained it will be possible to improve the resolution and wavelength range of this system.

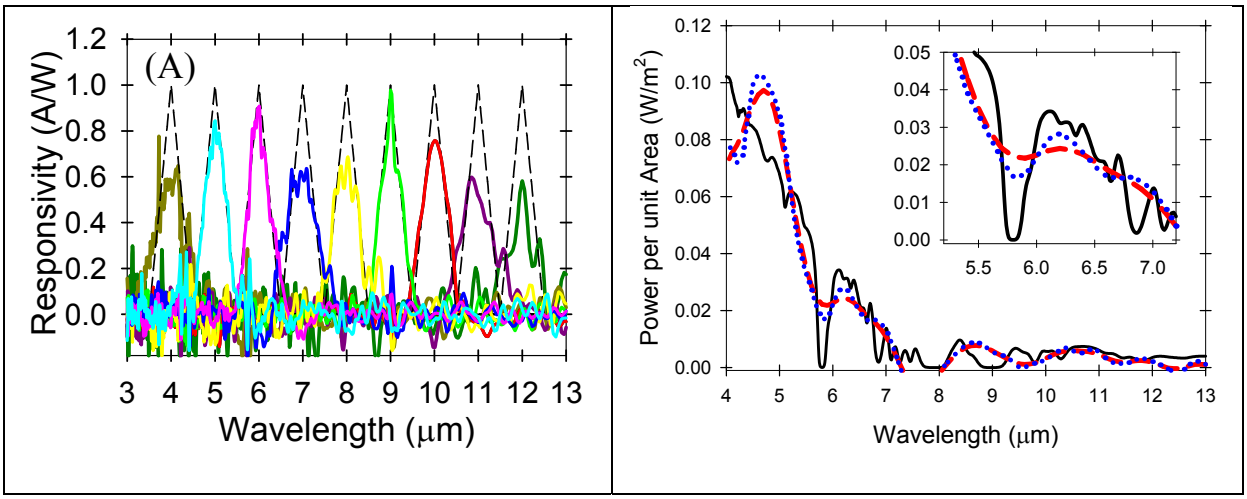

Figure 1. (Left) Synthesised spectral filters generated from the intrinsic spectral responses of a multi band QDIP combined with a post processing algorithm. (Right) Reconstruction of a polyethylene sheet spectrum (black solid line) using these filters. Reproduced from reference [7].

Table 1. Comparison of key distinguishing features and performance metrics for QDIP FPAs found in the general scientific literature

Paper and Group	Structure details	Array dimensions and operability	Temp.(K)	Wavelength range	D* ($cmHz^{1/2}/W$)	NETD (mK)	NEP ($W.Hz^{-0.5}$)
Krishna et al., 2005. [8] University of New Mexico, USA	15 period InAs-InGaAs-GaAs DWELL structure GaAs substrate	320x256 pixels 30µm pitch >99% operability	78K	MWIR LWIR	$7.1x10^{10}$ $2.6x10^{10}$ (single pixel)	<100mK f/1 <100mK f/2	$4.2x10^{-14}$ $1.1x10^{-13}$
Gunapala et al., 2007. [9] Jet Propulsion Laboratory, USA	30 period InAs-$In_{0.12}Ga_{0.88}As$- GaAs DWELL structure GaAs substrate	640x512 pixels 25µm pitch 23x23µm devices >99%operability	60K	LWIR 8.1µm peak	$~1x10^{10}$	40mK f/2 optics t=20ms	$2.3x10^{-13}$
Tsao et al., 2007. [10] Northwestern University, USA	25 period InAs-InGaAs-AlInAs DWELL structure InP substrate	320x256 pixels 30um pitch 25x25µm devices 99% operability	120-200K	MWIR Peak at 4µm	$<1x10^{10}$ single pixel at 120K at >-2V	344mK at 120K f/2 optics t<30ms	$2.5x10^{-13}$
Vaillancourt et al., 2009. [11] UMass + QmagiQ, USA	10 period InAs QD-$In_{0.2}Ga_{0.8}As$ barrier structure followed by 10 period InAs QD-GaAs barrier structure. GaAs substrate	320x256 pixels 30µm pitch 28x28um devices	67K	MWIR LWIR	$1.8x10^{9}$ single pixel	172mK f/2.2 t=16.7ms	$1.6x10^{-12}$
Nagashima et al., 2009 [12] Ministry of Defence, Japan + Fujitsu, Japan	10 period InAs QD-$Al_{0.15}Ga_{0.85}As$ barrier structure GaAs substrate	256x256 pixels 40µm pitch >99.5% operability	80K	LWIR 10.3µm peak		87mK t=8ms, f/2.5 optics	
Andrews et al., 2011 [13] Naval Research Laboratory, USA + University of New Mexico + QmagiQ, USA	30 period InAs-$In_{0.15}Ga_{0.85}As$-GaAs-$Al_{0.1}Ga_{0.9}As$ intermediate double DWELL structure, GaAs substrate	320x256 pixels 99.9% operability	60K	LWIR		106mK f/2 optics	
Lu et al., 2008 [14] UMass + Raytheon, USA	10 period InAs QD-$In_{0.2}Ga_{0.8}As$ barrier structure followed by 10 period InAs QD-GaAs barrier structure. GaAs substrate	320x256 pixels 30µm pitch 27x27µm devices >90% operability		LWIR	$2.3x10^{10}$ Single pixel		$1.2x10^{-13}$
Tang et al., 2006 [15] Chung-Shan Institute of Science and Technology, Taiwan	30 period InAs QD- GaAs barrier structure GaAs substrate	256x256 pixels >98% operability	80K	MWIR LWIR	$1.5x10^{10}$ Single pixel	Not given	
Barve et al., 2011 [16] University of New Mexico, USA	30 period InAs-$In_{0.15}Ga_{0.85}As$- $Al_{0.08}Ga_{0.92}As$ DWELL structure GaAs substrate	320x256 pixels	80K	6.1µm peak	$~4x10^{11}$ Single pixel	40mK f/2 optics	
Gunapala et al., 2011. [17] Jet Propulsion Laboratory, USA	Sub-ML InAs QD, GaAs QWs and AlGaAs barriers. GaAs substrate	1024x1024 pixels 19.5µm pitch	50K 60K 70K	8.5µm peak		22mK at 50K 28mK at 60K 33mK at 70K	

3. Summary of Type-II superlattice detector technology

3.1. Current performance and future potential

The historical and recent advances of single-pixel T2SL detectors and FPAs operating in the MWIR, LWIR and VLWIR windows have been reviewed. In Table 3 we present a summary of recent performance data for T2SL arrays (see RD-5 for full information).

Table 2 summarises the state-of-the-art performance figures of T2SL single-pixel and FPA detectors.

Table 2. Present state-of-the-art performance figures of T2SL detectors (at 77-80K).

Detector Type	Window	R_0A or R_dA (Ω cm^2)	D^* (Jones)
Single-pixel devices	MWIR	>3×10^7 [18]	8×10^{13} [18]
	LWIR	~1×10^4 [19] – NIP 1.4×10^4 [20] – CBIRD	>1×10^{12} [21]
	VLWIR	0.55 [22] – NIP 837 [23][68] – InAs/GaInSbN T2SL	4.5×10^{10} [21]
Focal plane array	MWIR	2.3×10^7 [24]	>1×10^{13} [25, 26]
	LWIR	> 1×10^4 [27]	~1×10^{12} [28, 29]

Large-format T2SL FPAs (up to 1024×1024 pixels) capable of operating on sub-millisecond time scales have been achieved. Further increase in array dimensions is presently limited by the commercial availability of larger-sized GaSb substrates. This can be circumvented by lattice mismatched epitaxial growth of T2SL on GaAs or even Si substrates, although the large lattice mismatch between T2SL and GaAs or Si makes eliminating dislocations in the T2SL active region challenging. T2SL FPAs are now commercially available (AIM-Infrarot), and several groups have developed nearly commercial-ready prototypes. The Fraunhofer IAF, Jet Propulsion Laboratory and Northwestern University groups have consistently demonstrated state-of-the-art T2SL FPA performance through high-quality fabrication processes and innovative device designs.

The electrical performance of liquid-N_2 cooled T2SL detectors is approaching that of HgCdTe, especially at LWIR wavelengths. Although the T2SL material system has the potential for realising high-operating-temperature (HOT) MWIR T2SL detectors, they are more difficult to achieve due to the effect of defects on the leakage current and minority carrier lifetime. Optimising the material quality for HOT applications should typically enhance the device performance at low temperatures. At present, the lack of progress in improving bulk T2SL material quality raises concern about the prospects for continued advancement in T2SL detector performance. Much of the advancement so far can be attributed to design workarounds, where the goal is to block the dark current using barrier structures while allowing the flow of photocurrent, rather than eliminating defect-originated leakage currents from the bulk T2SL material itself.

Table 3. Recent results for T2SL arrays available from the open literature.

Date, Affiliation, Reference	Device Structure	*T* (K)	Bias (mV)	λ (μm)	QE	R_dA (Ω cm^2)	J_{dark} (A/cm^2)	D^* (Jones)	NETD (mK)	NEP (W.Hz$^{-0.5}$)	Array Dimensions and Operability
Jul. 2012 Jet Propulsion Laboratory [30] Rafol-JQE	- InAs/GaSb T2SL - *n*-type CBIRD structure.	78, 65	128	8.8 (50%)	**54% (max) @ 5.7 μm**	N/A	2.2e-4 @ 78K 1.1e-4 @ 65K	**1.3x10^{11} @ 78K** **1.6x10^{11} @ 65K**	**18.6 @ 78K** **12 @ 65K**	**2.1x10^{-16}** **1.7x10^{-16}**	- 320×256 pixels - Pixel size: 27μm - Pitch: 30μm - Fill factor: 81% - **QE operability: 97%** - Int. time: 0.37ms - 298K background, f/2 optics
May 2012 QmagiQ (US) [31] Sundaram-SPIE	- InAs/GaSb T2SL	77	**-25**	~9.5	**50% (mean)**	N/A	~2e-4	N/A	30		- **1024×1024 pixels** - **Pixel size: 16μm** - **Pitch: 18μm** - Pixel operability: 96% - f/4 optics
May 2012 Jet Propulsion Laboratory [32] Soibel-SPIE	- InAs/GaSb T2SL - *n*-type CBIRD structure.	77	**50**	10	**R: 2 A/W**	N/A	**<1e-5**	N/A	**26 @ 80K**		- 320×256 pixels - **Pixel operability: 98%** - 300K background
Jan. & Feb. 2012 Northwestern University [33, 34] Haddadi-JQE, SPIE	- InAs/GaSb T2SL - M-structure	68, 81	**20 (81K) 35 (68K)**	7.9	**81% (w/o AR coating, 81K)**	76 @ 81K 309 @ 68K	1.09e-3 (81K) 2.78e-4 (68K)	N/A	**27 @ 81K** **19 @ 68K**		- **1024×1024 pixels** - **Pitch: 18μm** - Fill factor: 71.3% - **QE operability: 95.8% (81K), 97.4% (68K)** - **Weak low-*f* noise.** - Frame rate: 15Hz - Dynamic range: 37dB (81K), 39dB (68K) - **Int. time: 0.13ms** - 300K background, f/2 optics - ICP etched, SiO_2 passivated.

Several preliminary studies have concluded that the T2SL material appears to have good radiation tolerance, making this material attractive for space applications. The radiation tests have so far been performed on single-pixel T2SL devices. No studies have yet been reported on the effects of radiation on the performance and uniformity of T2SL FPAs. Very little is known about the degradation of device structure and electrical properties with exposure to ionising radiation over a prolonged period of time.

In short, the inherent flexibility, uniformity, stability, and robustness of the T2SL material system are its major advantages over HgCdTe. Rapid advances have led to the demonstration of 1-megapixel FPA cameras from single-pixel devices in just over a decade. This progress has been significantly more rapid than that for QDIP development. Results to date indicate a promising potential for T2SL detectors to operate in space environments, especially in the LWIR and VLWIR windows.

4. Comparison of TIR detector technologies

In Table 4 we present a summary of indicative current state-of-the-art performance figures for infrared arrays based on different technologies. Among the alternative detector technologies, the InAs/GaSb (and related alloy) type-II superlattice has emerged as the most promising material system to achieve large-format FPAs with performance potentially surpassing that of HgCdTe, especially at extended wavelengths in the VLWIR region.

4.1. Cost

HgCdTe photodetectors are grown on CdZnTe substrates, which are much more expensive than the GaSb substrates typically used for T2SL. GaSb substrates are also available in larger sizes than CdZnTe, making it possible to realise lower cost megapixel T2SL FPAs. GaSb wafers with diameters up to 6” (152 mm) are commercially available, while the maximum size of CdZnTe substrate is 70 mm×70 mm.

Large-format FPAs are necessary to provide high resolution imaging over a large field of view. To produce large-format FPAs at the lowest cost, HgCdTe infrared detectors have been grown on alternative substrates such as Si and sapphire (Al_2O_3). In 2000, the world’s first 2048×2048 HgCdTe FPA, for use in astronomical applications, was grown on a 3” sapphire substrate [35]. Around the same time, Raytheon demonstrated a 640×480 HgCdTe FPA on a 4" Si substrate [36]. The biggest advantage of HgCdTe/Si is that it resolves the thermal mismatch between the substrate and the Si read-out integrated circuit (ROIC). However, the 19% lattice mismatch between HgCdTe and Si results in a threading dislocation density that is still at least an order of magnitude higher than that in HgCdTe grown on CdZnTe. In recent developments, Selex Galileo is now able to produce state-of-the-art arrays for both MWIR and LWIR wavebands using MCT growth on a GaAs substrate.

4.2. Uniformity

Uniformity still remains an issue with HgCdTe. Compositional non-uniformity, in particular, results in a variation of cut-off wavelengths and hence non-uniform detector response between individual pixels. Excellent temperature stability is required to minimise the bandgap variation between the centre and edge of a wafer for HgCdTe. In contrast, T2SL has a weaker bandgap dependence on composition, and hence less stringent requirements on growth temperature stability. Given the high performance specifications required for space applications, such pixel non-uniformity will lead to poorer wafer yields for HgCdTe.

It is obvious that achieving a highly uniform, large-area ternary substrate suitable for lattice matched growth, based on the $Cd_{0.96}Zn_{0.04}Te$ alloy is still a difficult challenge. T2SL structures, on the other hand, can be grown precisely lattice matched to GaSb substrates, since the two constituent layers are designed to be strain balanced. In the LWIR and VLWIR regions, HgCdTe FPAs are limited to small format due to the above mentioned uniformity

Table 4. Comparison of TIR technologies

Technology	Array size	Pitch (µm)	Operating Temp. (K)	Noise Performance	Integration Time	Optics	Wavelength	Dark Current	Quantum Efficiency
VLWIR HgCdTe	640x512	24	70	Mode NETD of 35mK	20 µs	f/2	7.5-14.8µm	Not quoted	61% median
MWIR HgCdTe [37]	2048x2048	15	78	23.1mK	Not quoted	Not quoted	3.5-6.0µm	$<10^{-5}$ A/cm^2	60%
QWIP [38]	1024x1024	30	68	MWIR NETD: 27mK LWIR NETD: 40mK	Not quoted	f/2	MWIR: 4.4-5.1µm LWIR: 7.8-8.8µm	Not quoted	4.6%
VLWIR QWIP [39]	640x512	25	35	NETD of 48mK	1ms	f/2	10.5-16µm Peak at 13.5 µm	Not quoted	9.5%
T2 SL [34]	1024x1024	18	81	NETD of 23.6 mK	0.13ms	f/4	11µm cut-off	$3.3x10^{-4}$ A/cm^2	45% at 10 µm
Micro Bolometer [40]	1024x768	17	293	NETD of 40mK	~10ms	f/1	Optimised for 8-14µm	Not quoted	Not quoted
QDIP	1024x1024	19.5	70	NETD of 33mK	Not quoted	f/2	8.5µm peak	Not quoted	Not quoted
InSb [3]	2048x2048	25	30	Read noise of 4e-	Not quoted	Not quoted	0.6-5.2µm	0.01 e-/pixel/s	90%
Extrinsic Si (BIB) [41]	1024x1024	25	7.1	Read noise of 10e-	Not quoted	Not quoted	5-26µm	0.1 e-/pixel/s	50-70% 30% above 24µm

issues. Additionally, for VLWIR operation at about 40 K, HgCdTe FPAs are subject to additional stress due to mismatch of the thermal expansion coefficient between the CdZnTe substrate and the ROIC chip. The challenges associated with extending large-format HgCdTe FPAs on CdZnTe substrate into the VLWIR region have driven efforts to develop alternative infrared materials, such as the T2SL, that have the potential for low-background VLWIR operation in space.

4.3. Dark current

It has been predicted that HgCdTe ideal diodes with a cut-off wavelength of 5 µm give nearly two orders of magnitude reduction of dark current compared with InSb [42]. However, a theoretical prediction by Klipstein *et al.* [43], concluded that for ideal diodes at a given bandgap, HgCdTe and InAsSb have no fundamental advantages over each other. The magnitude of the dark currents is mainly dictated by the material quality and uniformity. In practice, InAs/Sb materials, and related T2SL material combinations, have relatively weaker dependence of bandgap on composition and a high degree of structural uniformity, which give them a competitive edge over HgCdTe.

The zero-bias differential resistance-area product, R_0A, of various forms of HgCdTe, T2SL and InSb single-pixel devices as a function of the cut-off wavelength at 77K, has been compared, along with diffusion-limited theoretical prediction [43-45]. It is evident that the dark currents of T2SL devices approach those of HgCdTe, especially at longer wavelengths (> 8 µm). Considering the relatively short history of T2SL infrared detectors development, these results suggest that the performance of T2SL detectors may potentially exceed that of HgCdTe in future as a result of the reduction in dark current.

Currently, the dark current performance in T2SL detectors is primarily limited by technological issues. Although some studies have reported diffusion-limited dark currents at temperatures from room temperature down to 77 K [21, 46, 47], the mesa sidewalls are still a major contributor to excess currents especially at low temperatures, which affect the pixel uniformity and operability. Various potential passivation techniques have been studied for T2SL detectors [47-49], but the improvement demonstrated was often marginal and inconsistent, and there is not as yet an optimal passivation method that works irrespective of the T2SL structure and cut-off wavelength. An alternative workaround to eliminate surface leakage is to eliminate or reduce the exposed sidewall surface itself. The device structure can be designed with the bandgap graded to a larger value in the region with exposed sidewalls, to reduce the leakage current due to surface states [50], although this adds some complexity and therefore ultimately cost to the growth process.

4.4. Detectivity

The Johnson-noise limited detectivity, D^*, for a detector is a function of the R_0A and the quantum efficiency. The Johnson-noise limited D^* of T2SL is predicted to be up to an order of magnitude higher than that of HgCdTe [51]. However, the experimental D^* values of T2SL detectors reported so far are, at best, about an order of magnitude lower than the theoretically predicted and experimentally measured D^* for HgCdTe detectors. There is at least a two orders of magnitude room for improvement for the D^* of T2SL detectors at 77 K.

As the current detectivity performance of HgCdTe detectors has approached the theoretical prediction, the HgCdTe FPA development efforts are now primarily focused on improving the

uniformity and operability of the pixel array. For T2SL detectors, the detectivity performance has considerable room for improvement, and appears to be limited by two factors, namely high background carrier concentration and short minority carrier lifetimes [52]. The typical background concentration in T2SL LWIR devices is of the order of mid 10^{15} to low 10^{16} cm^{-3}. The lowest background concentration reported to date is 5×10^{14} cm^{-3} [53]. The T2SL material is known to suffer from short minority carrier lifetimes, which are typically in the tens of nanoseconds range. Recently, a breakthrough in minority carrier lifetime of close to half a microsecond has been reported for LWIR $InAs/InAs_{0.72}Sb_{0.28}$ T2SL [54]. This attests to the importance of continuous efforts in the optimisation of epitaxial growth to eliminate defects, especially at the superlattice interfaces.

5. Feasibility of using QDIP or T2SL arrays for satellite-based TIR focal plane arrays

An analysis of space instrument types which could benefit from QDIP or T2SL technology was presented. The sensitivity of these arrays is such that they find key utility for Earth observation or planetary science missions. They do not have the required sensitivity for general astronomy missions or exoplanet missions.

Using QDIP or T2SL arrays for scanning imaging multispectral radiometers as a direct replacement for existing HgCdTe devices could lead to a small number of advantages including greater FPA uniformity and stability as well as a longer system lifetime. In addition to this, there is potential for higher temperature operation if the growth and material challenges mentioned above can be overcome.

Pushbroom imaging multispectral radiometers would also benefit from QDIP or T2SL technology. Both technologies have the sensitivity to be used for these instruments, particularly T2SL, with NEPs in the region of $2x10^{-16}$ $WHz^{-1/2}$ being reported. There is potential for a novel compact non scanning hyperspectral imager if a QDIP FPA can be biased at different voltages, therefore exploiting QDIP's bias absorption edge tuneability. This could lead to a very compact multi-spectral pushbroom instrument. Further improvements in spectral resolution could be achieved using strip filters or a post processing algorithm.

The intrinsically narrow spectral response of QDIP FPA's at any single bias makes them unsuitable for Fourier transform spectrometers, scanning grating spectrometers and earth radiation budget radiometers.

Little space qualification work has been reported for QDIPs or T2SL. However due to extensive similarities with QWIPs - which are to be used in the forthcoming Landsat Data Continuity Mission – it is highly likely that QDIP FPAs will withstand the space environment and launch conditions.

T2SL devices are expected to have a certain tolerance to radiation as they contain Sb, which has a large atomic mass making Sb-based semiconductors less susceptible to displacement damage [55]. In the study by Weaver and Aifer from the Naval Research Laboratory (NRL), 88-period 13ML GaSb/0.5ML InSb/13ML InAs *p*- and *n*-type T2SL structures were irradiated with 1-MeV protons at room temperature [55]. It was found that the T2SL devices showed little degradation in QE, leakage current and activation energy at proton fluences below 5×10^{11} 1-MeV H^+/cm^2 (equivalent to a dose of ~1 Mrad(Si)). Above 1 Mrad(Si), degradation occurred in the form of reduced minority carrier lifetime

and increased surface leakage currents. Using 150 krad(Si) as the typical benchmark for radiation hardness, it can be concluded that the T2SL devices exhibit high radiation tolerance, making them attractive for space applications.

6. Technology roadmap

This section details a roadmap strategy for the realisation of full infrared camera systems based on focal plane detector arrays (FPA), for space applications. It considers FPAs based on both quantum dot infrared photodetectors (QDIP) and type two superlattices (T2SL). This roadmapping exercise is subtly different to other similar activities in other technology applications, in that the timeline for a viable technology normally sees a decrease in technology readiness level (TRL) as time extends out to the end goal, with increasingly uncertain or unexplored aspects to a full technology. **However**, both QDIP and T2SL technology are similar in interfacing and engineering to standard QWIP technology, where investment has been significant over the last 20 years, and also inherits substantial engineering benefit from existing IR detector programmes. The later technology incorporation is considered to be at a much greater TRL than the more immature fundamental device optimisation stages. These remain realistically at the low TRL 1-3 mark for fundamental materials aspects of research, even though reports of full FPA detectors are in the open literature. These are early demonstrators and significant optimisation is still possible.

For detectors based on these technologies to be realised and to be competitive, the potential for significant improvement in the FPA performance needs to be in evidence to justify diluting the limited production capability within the EU to invest and commit. Due to the evolutionary nature (a detector material change, but not a fundamental paradigm change in detection technique or in platform and supporting electronics), this is feasible for capabilities that have already successfully handled QWIP detectors. As such this is a relatively low risk engineering challenge so long as sufficient progress has been made with individual devices.

There are no ‘showstoppers’ to either of these technologies maturing into a viable IR detector technology, but considerable refinement may be necessary, particularly to individual layer and device design.

6.1. High-level pictorial roadmaps

Presented here (Figure 2, Figure 3) are simple high level roadmaps that are based on the standard ESA technology readiness level (TRL) status, coupled with a broad non-specific timeline. They are subdivided for convenience into separate areas of engineering and/or related physics challenges that could be addressed by leading research groupings. These can be considered as effective workpackages of a larger project to bring QDIP and T2SL technology to full camera status. The majority of consideration is based around a limited detector programme of say 50 detector arrays over a three year period, with associated basic research underpinning device progression.

An explanation of the “traffic light” indicators follows:

RED indicates that considerable work is needed if performance limits are to be reached within the section, and broadly this corresponds to TRL 1-3 in maturity. It should be stated that this does not

mean that rapid progress could not be made with targeted investment; however it may be considered to be a stumbling block, with no certainty of progress. Targeted work is needed.

AMBER indicates a higher readiness level (TRL4-6), very often through a large body of related work (eg. modelling for quantum dot laser structures and high efficiency LEDs), which gives considerable confidence that challenges can be overcome and progress can be made on a rapid timescale when necessary.

GREEN indicates a high TRL (7+), and indicates where there is minimal significant work necessary beyond what exists commercially, or exists as part of an existing national detector programmes. There are no foreseen barriers to delivery of a complete camera system from these GREEN highlighted activities.

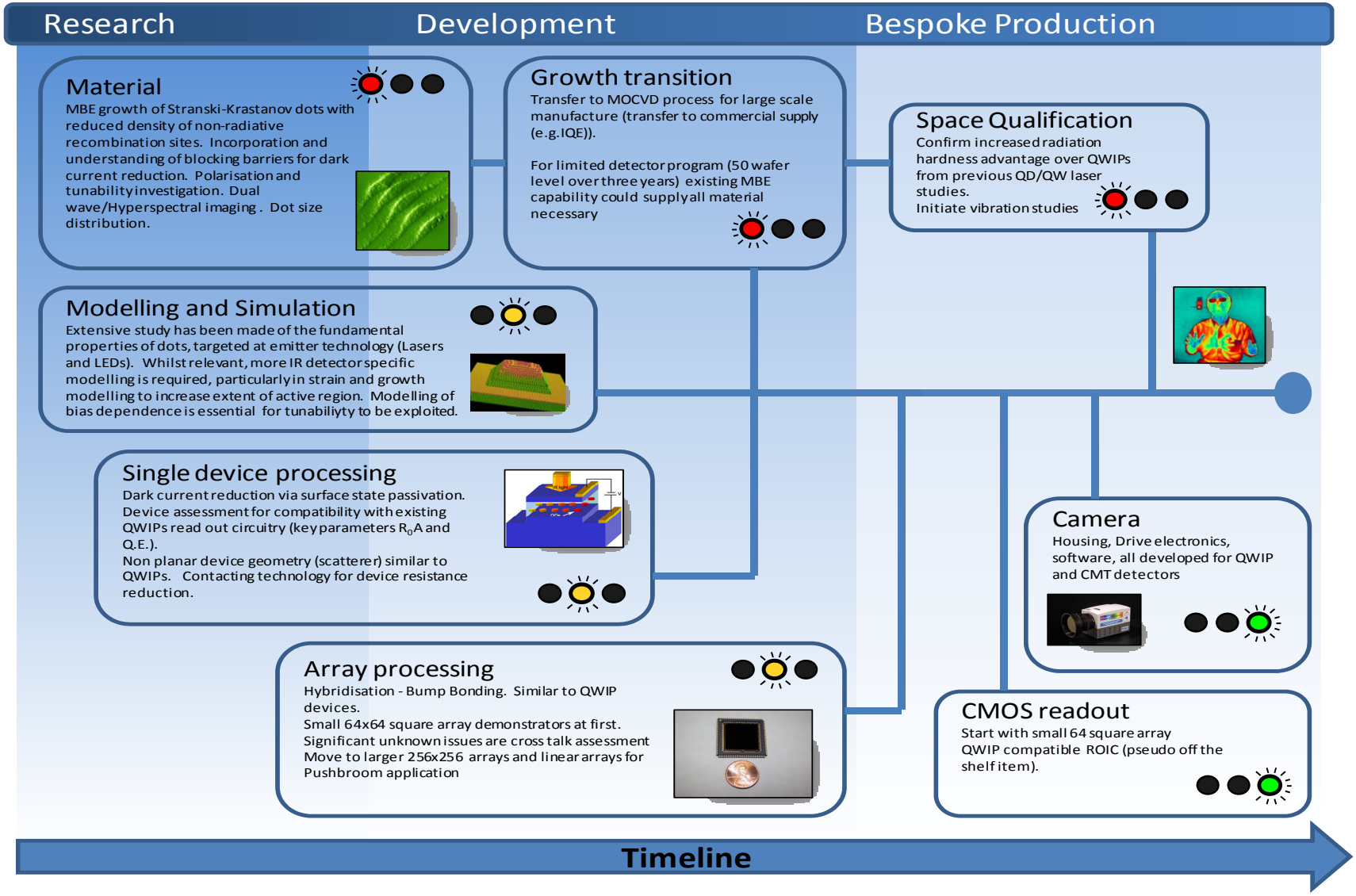

Figure 2. High level pictorial roadmap for QDIP detector array bespoke production (Limited run – 50 detector programme level). The timeline advances from left to right and has been left intentionally undefined as it is, to an extent, dependent on the intensity of future funding. A conservative estimate is that bespoke production (end of timeline), for space based application, is feasible within a 2-4 year time-frame.

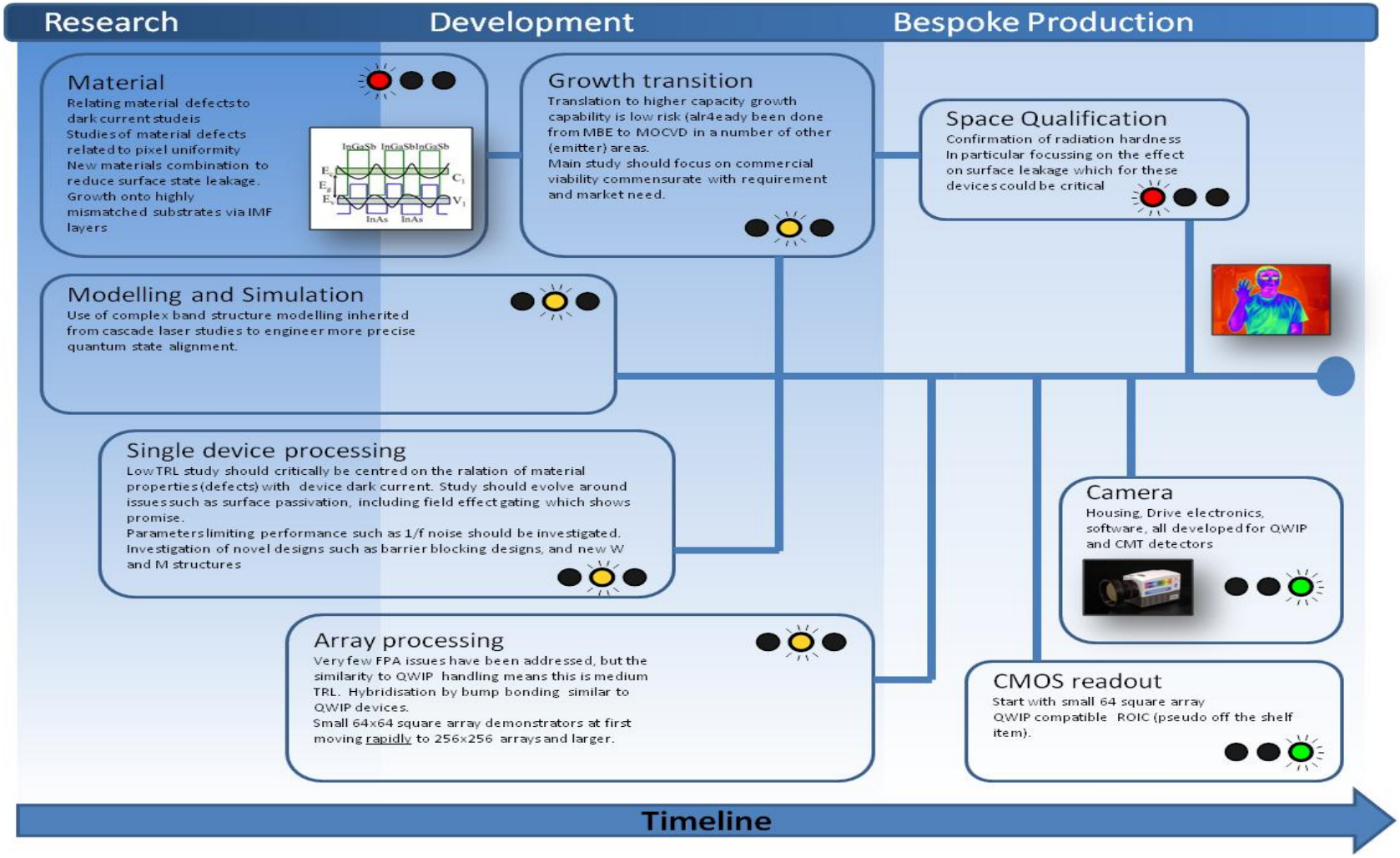

Figure 3. High level pictorial roadmap for T2SL detector array bespoke production (Limited run – 50 detector programme level). The timeline advances from left to right and has been left intentionally undefined as it is, to an extent, dependent on the intensity of future funding. A conservative estimate is that bespoke production (end of timeline), for space based application, is feasible within a 2-4 year time-frame.

6.2. Roadmapping summary

Compiled below are the main suggestions for focused study to realise high performance QDIP and T2SL detector arrays. These can be used in conjunction with the high level pictorial maps detailed in Figure 2 and Figure 3.

QDIPs

3.1	Material 1. Defect reduction research and understanding of non-radiative centres within the holding matrix, in particular time resolved luminescence measurements to study carrier relaxation mechanisms. 2. Demonstration of saturated dot layers where the recapture length is less than the total device active layer thickness. 3. Heterostructure engineering for resonant carrier escape mechanisms. 4. Possible investigation into other growth modes that are better suited to uniformity
3.2	Growth Transition 1. Assessment of requirement for commercial quantity.
3.3	Single Element Devices 1. Novel geometries to enhance in plane absorption, similar to grating structures in QWIPs. 2. Integration and investigation of Novel Plasmonic and Photonic Bandgap enhancement to absorption mechanisms (including the interaction of IR metamaterials with detector structures). 3. Comprehensive examination of dark current mechanisms, origins and physical control.
3.4	Theoretical Study and Device Modelling 1. Tailored modelling for strain compensation to increase dot absorption layers, specifically for IR absorption. 2. Specific modelling for plasmonic or metamaterial enhancement to detection process
3.5	Focal Plane Arrays 1. Cross talk studies of closely spaced (down to 15µm pitch) test arrays. 2. Quantitative study of Pixel Uniformity for large arrays (→1024x768)
3.6	Space Qualification 1. Confirming radiation hardness of these devices. 2. Initiate vibration study – expected to be the same as QWIPs
3.7	Hybridisation No Significant Issues with current COTS technology
3.8	Camera Electronics and Platform Housing No Significant Issues with current COTS technology

T2SLs

3.1	Material  1. The effect of dislocations on pixel operability and dark current 2. Defect reduction research and understanding of non-radiative centres, in particular time resolved luminescence measurements to study minority carrier relaxation mechanisms. 3. New strain relieving studies using IMF layers 4. New material combinations to reduce surface conduction states
3.2	Growth Transition  1. Assessment of requirement for commercial quantity.
3.3	Single Element Devices  1. Reliable device passivation to eliminate/minimise surface leakage currents (dark currents) 2. Develop novel mesa structures to minimise dark current/ sidewall leakage 3. Investigate and progress novel gated structures to minimise dark current/ sidewall leakage 4. Systematic study of 1/f noise in T2SL diodes
3.4	Theoretical Study and Device Modelling  1. Use band structure engineering developed for complex cascade laser designs to gain better predictive control of subband energies for complex T2 designs (such as W and M structures)
3.5	Focal Plane Arrays  1. Growth onto large format GaAs material to enable III-V foundry processing to be utilised routinely
3.6	Space Qualification  1. Confirming radiation hardness of these devices. 2. Initiate vibration study – expected to be the same as QWIPs
3.7	Hybridisation  No Significant Issues with current COTS technology
3.8	Camera Electronics and Platform Housing  No Significant Issues with current COTS technology

7. References

1. Phillips, J., *Evaluation of the fundamental properties of quantum dot infrared detectors.* Journal of Applied Physics, 2002. **91**(7): p. 4590-4594.
2. Martyniuk, P. and A. Rogalski, *Quantum-dot infrared photodetectors: Status and outlook.* Progress in Quantum Electronics, 2008. **32**(3): p. 89-120.
3. Hoffman, A.W., et al. *2K× 2K InSb for astronomy*. in *Proceedings of SPIE*. 2004.
4. Beletic, J.W., et al. *Teledyne imaging sensors: infrared imaging technologies for Astronomy & Civil Space*. in *Proc. SPIE*. 2008.
5. Rogalski, A., J. Antoszewski, and L. Faraone, *Third-generation infrared photodetector arrays.* Journal of Applied Physics, 2009. **105**(9): p. 091101-091101-44.
6. Jang, W.Y., et al., *Demonstration of bias-controlled algorithmic tuning of quantum dots in a well (DWELL) midIR detectors.* Quantum Electronics, IEEE Journal of, 2009. **45**(6): p. 674-683.
7. Vines, P., et al., *Versatile spectral imaging with an algorithm-based spectrometer using highly tuneable quantum dot infrared photodetectors.* Quantum Electronics, IEEE Journal of, 2011. **47**(2): p. 190-197.
8. Krishna, S., et al., *Demonstration of a 320× 256 two-color focal plane array using InAs/InGaAs quantum dots in well detectors.* Applied physics letters, 2005. **86**(19): p. 193501-193501-3.
9. Gunapala, S.D., et al., *640× 512 pixels long-wavelength infrared (LWIR) quantum-dot infrared photodetector (QDIP) imaging focal plane array.* Quantum Electronics, IEEE Journal of, 2007. **43**(3): p. 230-237.
10. Tsao, S., et al., *High operating temperature 320× 256 middle-wavelength infrared focal plane array imaging based on an InAs/InGaAs/InAlAs/InP quantum dot infrared photodetector.* Applied physics letters, 2007. **90**(20): p. 201109-201109-3.
11. Vaillancourt, J., et al., *A voltage-tunable multispectral 320× 256 InAs/GaAs quantum-dot infrared focal plane array.* Semiconductor science and technology, 2009. **24**(4): p. 045008.
12. Nagashima, M., et al. *High performance 256× 256 pixel LWIR QDIP*. in *Proc. of SPIE*. 2009.
13. Andrews, J.R., et al., *Comparison of Quantum Dots-in-a-Double-Well and Quantum Dots-in-a-Well Focal Plane Arrays in the Long-Wave Infrared.* Electron Devices, IEEE Transactions on, 2011. **58**(7): p. 2022-2027.
14. Lu, X., J. Vaillancourt, and M.J. Meisner. *A voltage-tunable multiband quantum dot infrared focal plane array with high photodetectivity*. in *Proceedings of SPIE, the International Society for Optical Engineering*. 2008. Society of Photo-Optical Instrumentation Engineers.
15. Tang, S.F., et al., *High-temperature operation normal incident 256× 256 InAs-GaAs quantum-dot infrared photodetector focal plane array.* Photonics Technology Letters, IEEE, 2006. **18**(8): p. 986-988.
16. Barve, A.V., et al., *High temperature operation of quantum dots-in-a-well infrared photodetectors.* Infrared physics & technology, 2011. **54**(3): p. 215-219.
17. Gunapala, S., et al., *Large area III–V infrared focal planes.* Infrared physics & technology, 2011. **54**(3): p. 155-163.
18. Hill, C.J., et al., *MBE grown type-II MWIR and LWIR superlattice photodiodes.* Infrared physics & technology, 2007. **50**(2): p. 187-190.
19. Wei, Y., et al., *High-performance type-II InAs/GaSb superlattice photodiodes with cutoff wavelength around 7 mu m.* Applied physics letters, 2005. **86**(9): p. 091109-3.
20. Ting, D.Z.Y., et al., *A high-performance long wavelength superlattice complementary barrier infrared detector.* Applied physics letters, 2009. **95**(2): p. 023508-023508-3.
21. Fuchs, F., et al., *High performance InAs/GaInSb superlattice infrared photodiodes.* Applied physics letters, 1997. **71**: p. 3251.
22. Wei, Y., et al., *Advanced InAs/GaSb superlattice photovoltaic detectors for very long wavelength infrared applications.* Applied physics letters, 2002. **80**(18): p. 3262-3264.

23. Aina, L., et al., *High detectivity dilute nitride strained layer superlattice detectors for LWIR and VLWIR applications.* Infrared physics & technology, 2009. **52**(6): p. 310-316.
24. Rehm, R., et al., *Dual-colour thermal imaging with InAs/GaSb superlattices in mid-wavelength infrared spectral range.* Electronics Letters, 2006. **42**(10): p. 577-578.
25. Walther, M., et al., *256× 256 focal plane array midwavelength infrared camera based on InAs/GaSb short-period superlattices.* Journal of Electronic Materials, 2005. **34**(6): p. 722-725.
26. Walther, M., et al., *Growth of InAs/GaSb short-period superlattices for high-resolution mid-wavelength infrared focal plane array detectors.* Journal of crystal growth, 2005. **278**(1): p. 156-161.
27. Rhiger, D.R., et al. *Characterization of barrier effects in superlattice LWIR detectors*. in *SPIE Defense, Security, and Sensing*. 2010. International Society for Optics and Photonics.
28. Huang, E.K., et al., *Type-II superlattice dual-band LWIR imager with M-barrier and Fabry–Perot resonance.* Optics Letters, 2011. **36**(13): p. 2560-2562.
29. Huang, E.K. and M. Razeghi. *World's first demonstration of type-II superlattice dual band 640x512 LWIR focal plane array*. in *Proceedings of SPIE*. 2012.
30. Rafol, S.B., et al., *Performance of a 1/4 VGA Format Long-Wavelength Infrared Antimonides-Based Superlattice Focal Plane Array.* Quantum Electronics, IEEE Journal of, 2012. **48**(7): p. 878-884.
31. Sundaram, M., et al. *1024x1024 LWIR SLS FPAs–Status and Characterization*. in *Proc. of SPIE Vol*. 2012.
32. Soibel, A., et al. *High-performance LWIR superlattice detectors and FPA based on CBIRD design*. in *Proceedings of SPIE*. 2012.
33. Haddadi, A., et al. *Low frequency noise in 1024× 1024 long wavelength infrared focal plane array based on type-II InAs/GaSb superlattice*. in *SPIE OPTO*. 2012. International Society for Optics and Photonics.
34. Haddadi, A., et al., *High Operability 1024 1024 Long Wavelength Type-II Superlattice Focal Plane Array.* IEEE Journal of Quantum Electronics, 2012. **48**(2): p. 221-228.
35. Cabelli, C.A., et al. *Latest results on HgCdTe 2048x2048 and silicon focal plane arrays*. in *Proc. SPIE*. 2000.
36. Varesi, J., et al., *Fabrication of high-performance large-format MWIR focal plane arrays from MBE-grown HgCdTe on 4 "silicon substrates.* Journal of Electronic Materials, 2001. **30**(6): p. 566-573.
37. Bangs, J., et al. *Large format high-operability SWIR and MWIR focal plane array performance and capabilities*. in *SPIE Defense, Security, and Sensing*. 2011. International Society for Optics and Photonics.
38. Gunapala, S.D., et al., *Demonstration of megapixel dual-band QWIP focal plane array.* Quantum Electronics, IEEE Journal of, 2010. **46**(2): p. 285-293.
39. Rafol, S., et al. *Characterization of QWIP (10-16 μm) broadband FPA*. in *Proceedings of SPIE*. 2003.
40. Black, S., et al. *Uncooled detector development at Raytheon*. in *SPIE Defense, Security, and Sensing*. 2011. International Society for Optics and Photonics.
41. Love, P.J., et al. *1024× 1024 Si: As IBC detector arrays for JWST MIRI*. in *Optics & Photonics 2005*. 2005. International Society for Optics and Photonics.
42. Kinch, M., *Fundamental physics of infrared detector materials.* Journal of Electronic Materials, 2000. **29**(6): p. 809-817.
43. Klipstein, P., et al. *Antimonide-based materials for infrared detection*. in *Proceedings of SPIE*. 2002.
44. Bajaj, J. *State-of-the-art HgCdTe infrared devices*. in *Symposium on Integrated Optoelectronics*. 2000. International Society for Optics and Photonics.

45. Fuchs, F., et al. *Optoelectronic properties of photodiodes for the mid-and far-infrared based on the InAs/GaSb/AlSb materials family*. in *Proc. SPIE*. 2001.
46. Johnson, J., et al., *Electrical and optical properties of infrared photodiodes using the InAs/Ga< inf> 1-x</inf> In< inf> x</inf> Sb superlattice in heterojunctions with GaSb.* Journal of Applied Physics, 1996. **80**(2): p. 1116-1127.
47. Hood, A., et al., *On the performance and surface passivation of type II InAs/GaSb superlattice photodiodes for the very-long-wavelength infrared.* Applied physics letters, 2005. **87**(15): p. 151113-151113-3.
48. Banerjee, K., et al., *Electrical characterization of different passivation treatments for long-wave infrared InAs/GaSb strained layer superlattice photodiodes.* Journal of Electronic Materials, 2009. **38**(9): p. 1944-1947.
49. Hood, A., et al., *Near bulk-limited R0A of long-wavelength infrared type-II InAs/GaSb superlattice photodiodes with polyimide surface passivation.* Applied physics letters, 2007. **90**(23): p. 233513-233513-3.
50. Vurgaftman, I., et al., *Graded band gap for dark-current suppression in long-wave infrared W-structured type-II superlattice photodiodes.* Applied physics letters, 2006. **89**(12): p. 121114-121114-3.
51. Grein, C., et al., *Long wavelength InAs/InGaSb infrared detectors: Optimization of carrier lifetimes.* Journal of Applied Physics, 1995. **78**(12): p. 7143-7152.
52. Bajaj, J., et al. *Comparison of type-II superlattice and HgCdTe infrared detector technologies*. in *Defense and Security Symposium*. 2007. International Society for Optics and Photonics.
53. Hood, A., et al. *Performance characteristics of high-purity mid-wave and long-wave infrared type-II InAs/GaSb superlattice infrared photodiodes*. in *Proc. SPIE*. 2006.
54. Steenbergen, E., et al., *Significantly improved minority carrier lifetime observed in a long-wavelength infrared III-V type-II superlattice comprised of InAs/InAsSb.* Applied physics letters, 2011. **99**(25): p. 251110-251110-3.
55. Weaver, B. and E. Aifer, *Radiation Effects in Type-Two Antimonide Superlattice Infrared Detectors.* Nuclear Science, IEEE Transactions on, 2009. **56**(6): p. 3307-3309.